

日本天文学会早川幸男基金応募申請書

2014年9月10日締切分

申請者氏名	石井彩子 (Ayako Ishii: 会員番号 5807)
連絡先住所	〒980-8579 宮城県仙台市青葉区荒巻字青葉 6-6-01 機械系 2号館 403号室 大西研究室
所属機関	東北大学
職あるいは学年(年齢)	D1: 学振(2014年9月10日現在 25才)
任期(再任昇格条件)	
電子メール	ishii@rhd.mech.tohoku.ac.jp
電話番号(FAX番号)	022-795-5854 (FAX: 022-795-5854)
渡航目的	研究集会での口頭発表(予定)
渡航先	Swift:10 Years of Discovery
講演・観測・研究題目	Radiative Transfer Analysis for Coupled Computation with Relativistic Hydrodynamics Relevant to GRB (予定)
渡航国または地域(期間)	イタリア(2014年12月1日~12月6日)
渡航確認資料	会議のプログラムおよび参加受付期間を示す資料
援助費目	全額 滞在費+参加登録料のみサポートの場合辞退
援助希望額合計	254400円(税など込)
内訳	航空運賃 131960円(スイスインターナショナルエアライ ンズ見積もり), その他: 仙台駅から成田空港までの新幹線 および電車代 24352円, フィウミチーノ空港から開催場所 最寄駅であるテルミニ駅までの電車代 1088円, 参加登録料 47600円(350ユーロ×為替レート), 滞在費 49400円(7480 ×5+2000×6(滞在地5泊6日))
領収書コピー	10月1日頃送付予定
他からの援助	交通費: 不採択時は自費, 滞在費+講演登録料: 不採択時 は自身の研究費
早川基金採択歴	なし
日本天文学会での発表	3回(うち筆頭発表者のもの3回)
査読論文(印刷中を含む)	1編(うち筆頭著者のもの1編)
他の添付資料	関連論文1編のコピー

(学生・院生の場合には、本申請に関して指導教員の了解をもらい、指導教員から直接、了解する旨のメールを送付してもらって下さい。可能な限り、下記の指導教員メールアドレスのアカウントから送付してもらって下さい。)

指導教員: 東北大学・准教授・大西直文

指導教員メールアドレス: ohnishi@rhd.mech.tohoku.ac.jp

1 渡航の主旨とその学問的意義

今回の渡航は、2014年12月にイタリアで開催される国際会議 Swift: 10 Years of Discovery への参加を目的とする。申請者は「Radiative Transfer Analysis for Coupled Computation with Relativistic Hydrodynamics Relevant to GRB」というタイトルで、東北大学工学研究科の大西直文准教授、早稲田大学理工学術院の山田章一教授、京都大学基礎物理学研究所の長倉洋樹研究員、および理化学研究所の伊藤裕貴研究員と共同研究を行ってきた成果について口頭発表を行う予定である。この国際会議は、ガンマ線バースト (GRB) の観測衛星 Swift が打ち上げられてから10年が経過したことを記念するものであり、活動銀河核 (AGN)、超新星爆発、パルサーといった関連するコンパクト天体にまで視野を広げ、それらに関する観測的および理論的な研究発表を募ったものである。

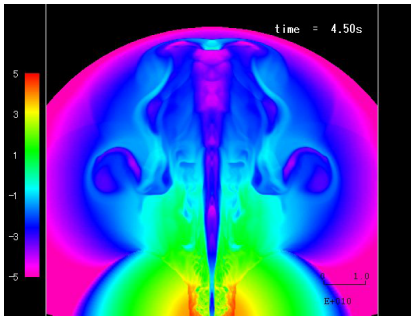


図 2: ジェットの内部構造.

申請者はこれまで、宇宙物理の最大の謎の一つである GRB のエネルギー放射メカニズムについて数値解析を行ってきた。特に高密度天体周辺で形成される相対論的ジェットを起源とする GRB 放射についてモデリングし、相対論的流体中における輻射輸送計算を取り扱ってきた。観測されている GRB のスペクトルは非熱的であり、図 1 のようにピークエネルギーを挟んで低エネルギー側と高エネルギー側で特徴的な傾きを持つ (Briggs et al. 1999)。このようなスペクトルを数値シミュレーション上で再現するために、ジェットの空間的構造をモデリングした定常バックグラウンド上で輻射輸送計算が行われてきた (Pe'er & Ryde 2011; Ito et al. 2013; Ito et al. 2014; Shibata et al. 2014)。

一方で、相対論的流体シミュレーションの結果より、図 2 のようにジェットの構造は多次元的であり、その内部構造が放射スペクトルに影響を与える可能性について示唆されてきた (Mizuta et al. 2006; Lazzati et al. 2009; Nagakura et al. 2011)。ジェット起源の GRB 放射を数値計算上で詳細に再現するためには、ジェットの多次元構造を考慮した非定常バックグラウンド上での輻射輸送計算が必要であり、すなわち相対論的流体と輻射輸送の結合計算が必要である。ここで述べている結合計算とは、バックグラウンドのジェットの流体計算を行い、そのバックグラウンド上で光の輸送を解き、光がジェット中の物質と相互作用を起こす場合には流体計算にそのフィードバックを取り入れるというものである。ここでは光をサンプル光子の集合として取り扱い、光子一つ一つについてそれぞれ輸送を計算する。このような結合計算では、輻射と物質との相互作用が強い場合から弱い場合まで同時に扱うことができる。非一様な密度分布を持つジェット中での光の輸送を精密に取り扱うためには結合計算が必要であるが、相対論的流体をバックグラウンドとした研究は世界的にもまだ行われていないため、計算手法について検証しておく必要がある。

申請者は、結合計算を目的とし、相対論的流体をバックグラウンドとする輻射輸送計算手法を検証しながら構築してきた。輻射輸送計算では、光子と物質の相互作用は流体静止系で取

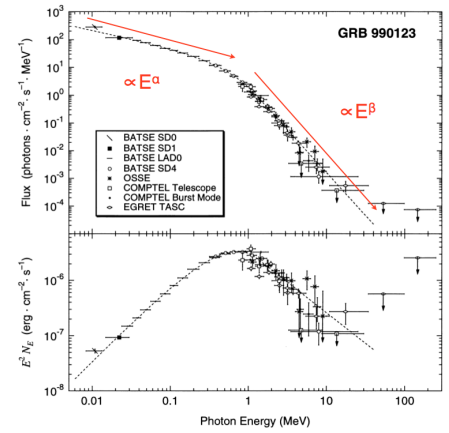


図 1: 観測から得られた GRB のスペクトル.

り扱い、輸送は観測者系で取り扱う必要があり、それらの慣性系の変換が計算中で度々繰り返されることになる。バックグラウンドが相対論的流体である場合であっても、この変換が矛盾なく取り扱えるような計算手法を構築するために、異なる慣性系で実行された輻射輸送計算の結果を同一の系で比較したとき同等の結果となるかを調べた。具体的には、相対論的 Rankine-Hugoniot の関係式から導いたある衝撃波について、衝撃波が静止している系と動いている系 (この時の衝撃波速度はローレンツファクター $\Gamma = 10, 100$ に相当) をそれぞれ準備し、各系においてそれぞれ輻射輸送計算を行い、放出される光子のスペクトルなどの計算結果を同一の系で比較することで、計算の妥当性を評価した。さらに、 $\Gamma = 100$ を越えるような超相対論的な流体場中の輻射輸送計算において信頼性の高い解を得るための計算条件について検証した。ここで、輻射輸送計算の手法としてはモンテカルロ法を用い、多数のサンプル光子について計算し統計的に輻射輸送方程式の解を得るものとした。

計算の結果得られたスペクトルを示す。図 3 は衝撃波静止系および衝撃波が $\Gamma = 10, 100$ で動いている系でそれぞれ輻射輸送計算を行った結果のスペクトルを示しており、また図 4 は各系におけるスペクトルをすべて衝撃波静止系に合わせて変換して表示したものである。図 3 ではスペクトルのピークエネルギーの位置がドップラーシフトによってずれているが、図 4 のように同一の系に合わせて変換すると一致することが確認できた。また、計算を行う際には流体バックグラウンド変化の時間間隔 Δt をある程度小さく刻む必要があり、その指標を算出した。さらに、図 4 において、光子エネルギーが 10 keV 以上の範囲に高エネルギー光子が分布している。これらの高エネルギー光子についてその軌跡とエネルギー変化を見たものが図 5 である。この図より、衝撃波下流側の比較的流速の緩やかな領域において放射された光子が衝撃波上流側の流速が極めて光速に近い領域へと輸送され、そこで相対論的電子に散乱されることによって高エネルギー光子が生成されていることを示しており、数値計算上で逆コンプトン散乱過程が再現されていることが確認できる。

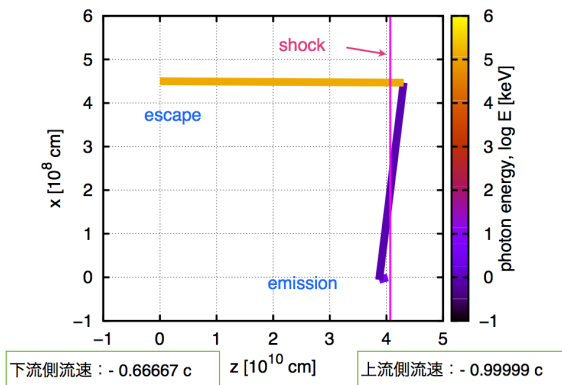


図 5: 高エネルギー光子の軌跡。

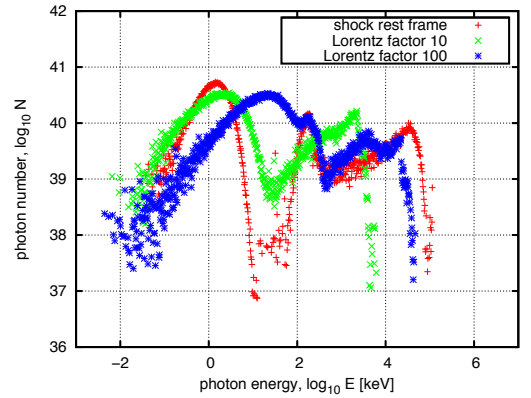


図 3: 各慣性系におけるスペクトルの比較。

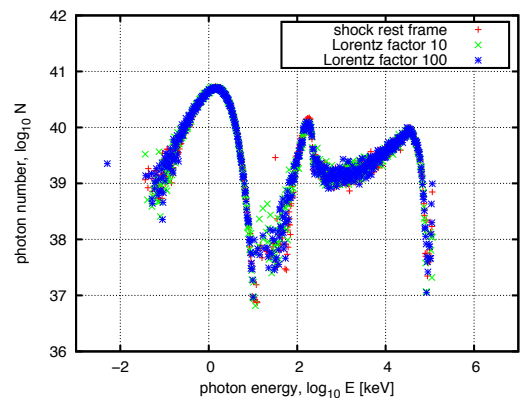


図 4: 各慣性系で計算した後同一の系に合わせて変換したスペクトルの比較。

申請者はこのように相対論的流体と輻射輸送の結合計算のための検証計算を行ってきた。これらの結果を GRB をはじめとする高エネルギー天体の専門家が集う国際会議の場で発表し、ジェット中の光の放射機構を詳細に取り扱える計算が実現可能であることを示し、それによって GRB 放射メカニズムが解明される可能性を示したいと考えている。また、専門家たちと有意義な議論を交わし、相対

論的流体-輻射輸送結合計算コードを開発した後に解析を進めていく高エネルギー天体現象について知見を得たいと考えている。

2 申請者の役割及び貢献度

申請者は、この国際会議で発表する予定の内容に関してこれまで中心となって研究を進めてきた。共同研究者たちと議論を交わし方針を固めた後は、申請者が主体となって数値計算コードを改変し計算結果を出してきた。本研究においては、相対論的流体と輻射輸送の結合計算を行うにあたり計算手法の妥当性を検証するというコンセプトは共同研究者との議論によって生まれたものだが、異なる慣性系をどのように準備するか、また空間および時間に関する計算条件をどのように決めるかといった詳細な計算内容は申請者によって構築された。計算を行う際の流体場の初期条件を決定する上で、共同研究者の先行研究のデータを参考にすることはあったが、その初期条件を用いて実際に計算を行ったのは申請者であり、開発している計算コードの中身についてもっともよく理解していると言える。これらのことから、この会議での発表内容に関しては申請者が筆頭著者を担っている。

3 今回の渡航に関する抱負あるいは成果

申請者は、今回の国際会議に参加し発表することにより、自身が構築している相対論的流体-輻射輸送結合計算の必要性について周知したいと考えている。GRBは発見以来四十年以上が経過しているにも関わらず、その詳細な放射メカニズムについては未だ解明されていない。宇宙物理の最重要課題の一つと言っても過言ではないこのテーマに関して、自身が行っている計算コード開発が解決の一端を担うことを主張したいと考えている。ジェット起源のGRBの放射機構を詳細に再現するためには相対論的非定常流体と輻射輸送の結合計算が必要であるが、この結合計算は世界的にも未踏の領域であり、本研究によりその実現可能性が示されたことは高エネルギー天体の分野において大きなインパクトを与えるものである。

今回の会議にはGRBの専門家も数多く参加しており、申請者の発表はそういった人々の注目を集めることが期待される。特に、講演者の一人であるDavide Lazzati氏は申請者と同じくジェット起源のGRBの数値シミュレーションを行っており、彼との議論は今後の計算コード開発の指針を決める上で大きく寄与することが予想される。また、申請者は数値シミュレーションコード開発を専門としているために、最新の観測結果について造詣が深いとは言えず、解析する対象の天体について情報収集する必要がある。今回の会議ではSwiftによる最新の観測結果についての講演が数多く予定されており、解析対象の情報収集には最適の機会である。相対論的流体と輻射輸送の結合計算はAGNや超新星爆発といったGRB以外の天体について放射メカニズムを調べる際の数値解析にも応用できるものであり、この会議において開発中のコードの応用可能性が広がることも考えられる。

以上のように、本国際会議においてGRB放射メカニズム解明に寄与するであろう相対論的流体-輻射輸送結合計算の実現可能性を示し、GRBをはじめとする高エネルギー天体の専門家たちと議論を交わすことにより、今後のコード開発や解析対象に関して新しいアイデアを得られると考えられる。ここで得られた知識や経験は今後の高エネルギー天体分野の発展に大きく寄与すると確信している。

4 申請者業績リスト

1. A. Ishii et al. (2013) *Parallel Computing of Radiative Transfer in Relativistic Jets Using Monte Carlo Method*: HEDP 9, 280
2. A. Ishii et al. (2014) *Identical Algorithm of Radiative Transfer Across Ultrarelativistic Shock in Different Inertial Frames*: HEDP (submitted)

[Welcome](#) [SOC & LOC](#) [Program](#) [Events](#) [Registration](#) [Where](#) [Accomodation](#) [Important dates](#)



Swift: 10 Years of Discovery

OVERVIEW


This meeting will celebrate 10 years of Swift successes and will provide the opportunity to review recent advances on our knowledge of the high-energy transient Universe both from the observational and theoretical sides.

When Swift was launched on November 20, 2004, its prime objective was to chase Gamma-Ray Bursts and deepen our knowledge of these cosmic explosions. And so it did, unveiling the secrets of long and short GRBs. However, its multi-wavelength instrumentation and fast scheduling capabilities made it the most versatile mission ever flown. Besides GRBs, Swift has observed, and contributed to our understanding of, an impressive variety of targets including AGNs, supernovae, pulsars, microquasars, novae, variable stars, comets, and much more. Swift is continuously discovering rare and surprising events distributed over a wide range of redshifts, out to the most distant transient objects in the Universe.

Such a trove of discoveries will be addressed in the upcoming Swift meeting with sessions dedicated to each class of events. The future prospects of time domain astrophysics, which could be addressed in the extended Swift mission, will be also reviewed.

Besides the classical Swift areas in time domain Astrophysics, contributions are solicited also in the following areas: new approaches on data analysis and theory as well as new ideas for non-conventional uses of the spacecraft.



 swift10years@brera.inaf.it

Program

Tuesday December 2, 2014

		Speaker	Title
			Swift and the future GRB missions
09.00	09.20	TBD	Welcome
09.20	09.50	Neil Gehrels	Swift results & Future
09.50	10.10	Alan Wells	Swift a historical view
10.10	10.30	Luigi Piro	Athena and GRBs
10.30	10.50	Lorenzo Amati	Possible future missions for GRBs within ESA
10.50	11.10	coffee break	
11.10	11.30	Josh Grindlay	Possible future missions for GRBs within NASA
11.30	11.50	Bertrand Cordier	The SVOM GRB mission
11.50	13.00	Paul O'Brien	Round table discussion on possible future mission for GRB studies
13.00	14.30	lunch	
			GRB I (physics: jets & progenitors)
14.30	15.00	Tsvi Piran	Prompt emission mechanisms
15.00	15.20	Davide Lazzati	Numerical simulations of GRB explosions
15.20	15.35	Hendrik van Eerten	A library of GRB afterglows: applicability and limitations
15.35	15.50	Contributed	
15.50	16.05	Contributed	
16.05	16.30	coffee break	
16.30	16.50	Klaas Wiersema	Polarization studies in GRB afterglows
			GRB II (high-z GRBs and cosmology)
16.50	17.20	Sandra Savaglio	GRB host galaxies
17.20	17.40	Ruben Salvaterra	The high redshift universe as probed by GRB
17.40	17.55	Contributed	
17.55	18.10	Contributed	
18.10	18.25	Contributed	
18.25	18.40	Contributed	

Wednesday December 3, 2014

		Speaker	Title
			GRB III (short GRBs)
09.00	09.30	Edo Berger	Short GRBs: a review
09.30	09.50	Giancarlo Ghirlanda	Are Short GRBs similar to long GRBs?
09.50	10.05	Contributed	
10.05	10.20	Contributed	
10.20	10.35	Contributed	
10.35	11.00	coffee break	
11.00	11.30	Enrico Ramirez-Ruiz	Short GRB models
11.30	11.50	Derek Fox	The ambient medium surrounding short GRBs
11.50	12.05	Contributed	
12.05	12.20	Contributed	

12.20	12.35	Contributed	
12.35	12.50	Contributed	
12.50	14.30	lunch	
Low luminosity - Very Long GRBs			
14.30	15.00	Re'em Sari	Low luminosity GRBs and shock break outs
15.00	15.20	Andrew Levan	Very long GRBs: a new class?
15.20	15.35	Contributed	
15.35	15.50	Contributed	
15.50	16.05	Contributed	
16.05	16.30	coffee break	
GRB-SNe connection			
16.30	17.00	Alicia Soderberg	GRB-SN connection: the Swift view
17.00	17.20	Thomas Janka	GRB-SN explosions: a theory primer
17.20	17.35	Contributed	
17.35	17.50	Contributed	
17.50	18.05	Contributed	
18.05	18.20	Contributed	
18.20	18.35	Contributed	
18.35	18.50	Contributed	

Thursday December 4, 2014

		Speaker	Title
Magnetar			
09.00	09.30	Chryssa Kouveliotou	An observational view of magnetars
09.30	09.50	Rosalba Perna	GRB and magnetars: observational predictions
09.50	10.05	Contributed	
10.05	10.20	Contributed	
10.20	10.35	Contributed	
10.35	11.00	coffee break	
Supernovae			
11.00	11.30	Peter Brown	Swift UVOT Ultraviolet Observations of Supernovae: Past, Present, and Future
11.30	11.50	Avishay Gal-Yam	Very luminous SNe (with GRBs?)
11.50	12.05	Contributed	
12.05	12.20	Contributed	
12.20	12.35	Contributed	
12.35	12.50	Contributed	
12.50	14.30	lunch	
Compact objects and the Galactic center			
14.30	14.50	Julian Osborne	Swift view of Novae
14.50	15.10	Jamie Kennea	X-ray transients with Swift
15.10	15.30	Nathalie Degenaar	The galactic center
15.30	15.45	Contributed	
15.45	16.00	Contributed	
16.00	16.30	coffee break	

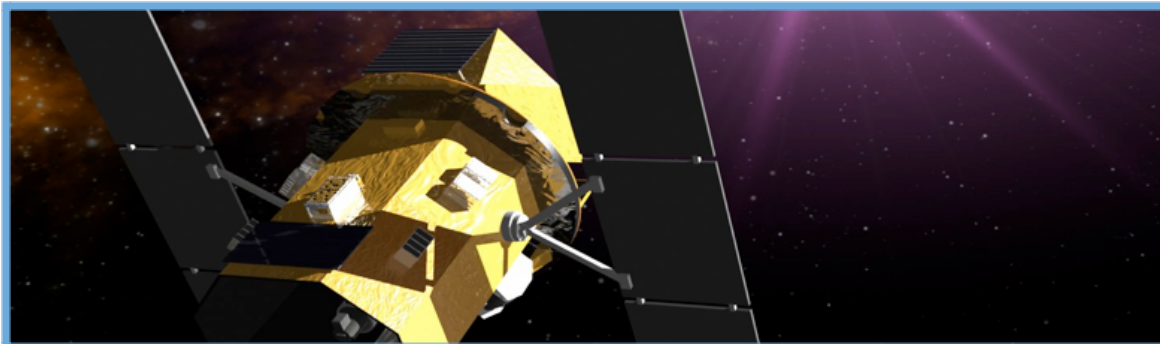
Swift catalogs

16.30	16.50	Richard Mushotzky	Results from the BAT catalog
16.50	17.10	Phil Evans	The XRT catalogs
17.10	17.30	Mathew Page	The UVOT catalogs
17.30	17.45	Contributed	
17.45	18.00	Contributed	
18.00	18.15	Contributed	
18.15	18.30	Contributed	
18.30	18.45	Contributed	

Friday December 5, 2014

		Speaker	Title
			Tidal Disruption
09.00	09.30	Stefanie Komossa	TDE: observational status
09.30	09.50	Giuseppe Lodato	TDE: theory and rates
09.50	10.05	Contributed	
10.05	10.20	Contributed	
10.20	10.35	Contributed	
10.35	11.00	coffee break	
			AGN - Blazar
11.00	11.30	Gabriele Ghisellini	Swift and the blazars
11.30	11.50	Jonathan McKinney	The central engine
11.50	12.05	Contributed	
12.05	12.20	Contributed	
12.20	12.35	Contributed	
12.35	14.00	lunch	
			Multiwavelength - Multimessengers
14.00	14.20	Paolo Giommi	The Swift contribution to multiwavelength campaigns
14.20	14.40	Eli Waxman	GRBs and neutrino astronomy
14.40	15.00	Fulvio Ricci	The detection of GW from transients: the future with Ligo and Virgo
15.00	15.20	Dieter Hartmann	Concluding remarks

[Welcome](#) [SOC & LOC](#) [Program](#) [Events](#) [Registration](#) [Where](#) [Accomodation](#) [Important dates](#)



Important Dates

- ▶ May 15, 2014: First Circular
- ▶ July 14, 2014: Second Circular and [Registration open](#)
- ▶ September, 30, 2014:



- Deadline for the abstract and poster submission
- Last day for early bird congress fee € 300,00 **without** Social Dinner and 350,00 **with** Social Dinner



- ▶ October 30, 2014:

- Final program

- ▶ November 14, 2014:

- Last day for reduced congress fee € 350,00 **without** Social Dinner and 400,00 **with** Social Dinner

From November, 15 the fee will be € 400,00 **without** Social Dinner and 450,00 **with** Social Dinner

▶ **December 2 - 5, 2014: Conference**

 swift10years@brera.inaf.it





Registration and Conference Fee

[How to Register](#)

To register, please follow these 3 steps

1. Fill in the [Registration form](#);
2. Complete the registration fee payment by [bank transfer](#) or [credit card](#) (please pay attention to select the right conference);
3. E-mail us a copy of the payment swift10years@brera.inaf.it

[Deadline for abstract submission is September, 30, 2014.](#)

[Conference Fee](#)

	Conference Fee without Social Dinner	Conference Fee with Social Dinner
early bird fee	300,00 Euro up to September, 30, 2014	350,00 Euro up to September, 30, 2014
reduced fee	350,00 Euro up to November, 14 2014	400,00 Euro up to November, 14 2014
full fee	400,00 Euro after November, 14 2014	450,00 Euro after November, 14 2014

The registration fee includes all **lunches** for four days, coffee breaks, conference documents.

The Social Dinner you should be requested in the registration form and the corresponding amount has to be paid together with the fee.

[Registration form](#)

[Credit Card Form](#) please pay attention to select the right conference and the social dinner option (w or w/o)

Bank

Cancellation Policy

If you decide to cancel your participation before August 30, 2014 the registration fee will be refunded deducting a 30% handling fee. Between September 1, 2014 and October 31, 2014 a 50% cancellation fee will be applied. After November 1, 2014 there will be no refund whatsoever.

Cancellations must be communicated in written form via e-mail to swift10years@brera.inaf.it with all details needed for the refund.

Further information

Should you have any special request for the processing of your invoice, kindly let us know via [e-mail](#).

In case you need a letter of invitation please send us an e-mail to swift10years@brera.inaf.it

 swift10years@brera.inaf.it





東京（成田国際空港）発 ローマ行き海外航空券/格安航空券 予約内容確認

ご予約はまだ完了していません。（予約の確保は予約完了時となります）

空席状況は常に変化しますので、内容を十分にご確認の上、お早めに次へ進んでください。

料金詳細

航空券代金	大人1名、子供0名、幼児0名	¥131,960 (内訳)
合計		¥131,960
ご請求額		¥131,960

フライト詳細

スイスインターナショナルエアラインズ (スターアライアンス加盟)		商品番号: LXNNEP8H
可能な旅行日数: 5日以上-21日以内		
<input type="checkbox"/> 正規割引		
往路 (行き) 2014/12/01 東京		
LX161 便 エコノミークラス	12/01 11:10 発 東京 (成田国際空港)	15:50 着 チューリッヒ (チューリヒ空港)
		乗継時間 1時間45分
LX1732 便 エコノミークラス	12/01 17:35 発 チューリッヒ (チューリヒ空港)	19:05 着 ローマ (レオナルドダビンチ/フィウミチーノ空港)
復路 (帰り) 2014/12/06 ローマ		
LX1727 便 エコノミークラス 運航: エアデルワイスイア	12/06 09:45 発 ローマ (レオナルドダビンチ/フィウミチーノ空港)	11:30 着 チューリッヒ (チューリヒ空港)
		乗継時間 1時間30分
LX160 便 エコノミークラス	12/06 13:00 発 チューリッヒ (チューリヒ空港)	08:55(+1日) 着 東京 (成田国際空港)

フライトを変更・キャンセルされる場合

[折りたたむ](#)

キャンセル料発生日: お支払手続き完了日 (※クレジットカードの場合、ご予約完了時に即支払い完了となります)

キャンセル料内訳: (1) 取消料 + (2) 取消事務手数料 + (3) 航空券取扱手数料の合計額が必要となります

- (1) = 航空会社、ホテルが定める取消料
 - (2) = 弊社の取消事務手数料 (お一人様 航空券 6,000円 + 消費税、ホテル2,000円 + 消費税)
※旅行代金ご入金後のお取消の場合、取消料発生日前であっても必要です。
 - (3) = 航空券取扱手数料 (お一人様につき)
- ※取消料は、大人一人あたり50,000円となります。
※取扱手数料は返金いたしません。

航空券ルール

[折りたたむ](#)

必要旅行日数	5日以上 - 21日以内
変更・取消料	大人 50,000円にて取消可

こちらから予約手続きへ進んでください

ご予約の際にご用意ください

ご旅行者全員分のパスポート名が確認できるもの
代表者の方の住所・電話番号

会員の方

既に会員登録をされている方は、メールアドレス (会員ID) とパスワードを入力してください。

登録メールアドレス(会員ID) 半角英数字

初めてご予約の方

ご予約には「会員登録 (無料)」が必要です。
ご予約と同時に会員登録となります。

メールアドレス(会員ID用) 半角英数字

以下のサイトID でログインして、予約申込みすることも可能です。



[Welcome](#) [SOC & LOC](#) [Program](#) [Events](#) [Registration](#) [Where](#) [Accommodation](#) [Important dates](#)



HOTELS

The workshop will be held at La Sapienza University nearby Roma Termini - the main train station of Rome.

In Rome there are many possibilities to find an hotel, so we did not make any particular effort to book an hotel.

However, we contacted the [Dreamtour Italy agency](#) that has pre-booked for us some rooms at special rates for the period December 2 - 4 in hotels close to the Conference venue (see list below). Rooms will be kept up to November, 15, 2014.

If you want to take advantage of this offer, please contact the agency directly. Please note that we have no responsibility for this service.

Hotel list is included below; it comprises 4-star and 3-star hotels. All hotels have internet point connection either in the rooms or in public areas.

Considering the high number of tourists usually visiting Rome, we strongly suggest you to book your room as soon as possible.

4 stars:

[HOTEL VILAFRANCA, Via Villafranca 9 - Roma](#)

DSU € 105,00

[HOTEL TORINO, Via Principe Amedeo 8 - Roma](#)

Single € 70,00 / DSU € 80,00

[HOTEL GALLIA, Via Di Santa Maria Maggiore 143 - Roma](#)

Single € 70,00 / DSU € 80,00

[HOTEL VIMINALE, Via Cesare Balbo 31 - Roma](#)

Single € 70,00 / DSU € 80,00

3 stars:

[HOTEL BRASILE, Via Palestro 13 - Roma](#)

Single € 70,00 / DSU € 85,00

[HOTEL WINDROSE, Via Gaeta 39 - Roma](#)

Single € 60,00 / DSU € 70,00

[HOTEL DANIELA, Via Luzzatti 31 - Roma](#)

Single € 55,00 / DSU € 70,00

[HOTEL FIAMMA, Via Gaeta 61 - Roma](#)

[HOTEL FIAMMA, Via Gaeta 01 - Roma](#)

Single € 55,00 / DSU € 70,00

[HOTEL SIVIGLIA, Via Gaeta 12 - Roma](#)

Single € 55,00 / DSU € 70,00

[HOTEL CAMELIA, Via Goito 36 - Roma](#)

Single € 90,00 / DSU € 105,00

[HOTEL PORTAMAGGIORE, P.zza di Porta Maggiore 25 - Roma](#)

Single € 60,00 / DSU € 70,00

[HOTEL BLED, Via Santa Croce in Gerusalemme 40 - Roma](#)

Single € 55,00 / DSU € 70,00

Note: DSU is double for single use

Requests for reservation must be sent directly to Dreamtour Italy via e-mail providing the information listed below (m.pizzichemi@dreamtour.it).

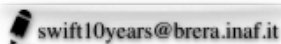
- ***Dates of your arrival and departure***
- ***Single room or double room for single use***
- ***Name and Surname***
- ***The Hotel you would like (please indicate at least 3 preferences)***
- ***Number and expiration date of your credit card***

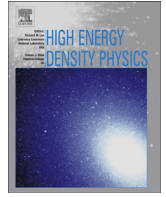
The reservation will be done on a first come first served basis. If the required hotel will not be available, the agency will suggest a similar hotel in the same area.

The indicated rates are per room and include breakfast, service charge and taxes (but not the city tax that amounts to 2 € /day for a 3-star hotel, 3 € /day for a 4-star hotel per person).

The payment will be due directly to the hotel upon departure, but a credit card is needed as a guaranty for the reservation.

Please, contact m.pizzichemi@dreamtour.it for any further information.





Parallel computing of radiative transfer in relativistic jets using Monte Carlo method



Ayako Ishii^a, Naofumi Ohnishi^{a,*}, Hiroki Nagakura^b, Hirotaka Ito^c, Shoichi Yamada^b

^aDepartment of Aerospace Engineering, Tohoku University, Sendai 980-8579, Japan

^bAdvanced Research Institute for Science and Engineering, Waseda University, Tokyo 169-8555, Japan

^cYukawa Institute for Theoretical Physics, Kyoto University, Kyoto 606-8502, Japan

ARTICLE INFO

Article history:

Received 13 June 2012

Received in revised form

21 December 2012

Accepted 3 January 2013

Available online 1 February 2013

Keywords:

Gamma-ray burst

Relativistic jet

Radiative transfer

Monte Carlo method

ABSTRACT

We present numerical attempts of radiative transfer in a relativistic scattering flow that can produce gamma rays using a three-dimensional Monte Carlo code. We prepared an initial background flowfield obtained from hydrodynamical simulation of a relativistic jet in which Thomson scattering dominates compared to absorption, and solved the radiative transfer equation for the background evolved by a simple expansion model. Since a large number of sample particles is required for an accurate computation, we have parallelized the Monte Carlo code in order to obtain solutions in a practical computational time even for a long-term simulation coupled with a time-dependent flowfield. Using this code, higher parallel efficiency is achieved with larger number of particles. The obtained light curve from the simple model shows a signal of the transition from the opaque post-shock flow to the transparent regime as the flow expands, and the high-energy photons are generated by not only the Doppler boosting but also the inverse Compton scattering.

© 2013 Elsevier B.V. All rights reserved.

1. Introduction

Origin of gamma-ray bursts (GRBs) has intensively investigated by many authors, so far. Although it is considered that GRBs are associated with formation of a black hole caused by neutron star merger [1] or with hypernovae that is much more luminous and energetic than ordinary supernovae (SNe) [2], the issue how GRBs are produced is still controversial. There is also an observational evidence that links at least some GRBs to core-collapse SNe [3]. SNe are commonly expected to be a feasible candidate creating such huge energy; however, it is difficult to discuss in terms of energy generation because of their isotropic energy emission [4]. On the other hand, around collapsing massive stars, directional flows within narrow area are formed with extremely high velocity approaching to almost speed of light [5–7]. Such collimated flows are called relativistic jets. Relativistic jets are also thought to play important roles on GRBs because it is easier to discuss about problems of energy generation if GRBs are emitted by the collimated relativistic flow [4].

Multi-dimensional dynamics of relativistic jets has been numerically investigated through an envelope of collapsing

massive star in the context of GRBs [5,8,9]. The jet propagation beyond a stellar surface has been simulated with an inference that a hot jet produces very bright photospheric emissions yielding a high radiative efficiency in the prompt phase of GRBs [10,11]. The radiative efficiency of the prompt GRBs may be also explained by taking into account pair photospheres and pair annihilation lines [12]. Recently, the photospheric emissions were identified for some long-duration GRBs [13,14]. Moreover, in spite that the locally emerging photons are thermal even in relativistic flows, since an observer simultaneously sees photons emitted from different angles, hence with different Doppler boosting, the observed spectrum becomes a multicolor blackbody [15].

A Monte Carlo technique is useful for dealing with propagation of photons, and emissions of X-ray and gamma ray can be discussed in a relativistic flow using this technique [16–18]. Although three-dimensional Monte Carlo simulation has been performed in the context of SNe [16,18], a comprehensive assessment for GRB origins needs a coupling computation with the relativistic jet dynamics. However, in order to take into account multi-dimensionally astrophysical phenomena, we generally require huge computational cost. So, we have developed a parallelized Monte Carlo code for solving the radiative transfer equation, which can be coupled with relativistic flow computation. Some test computations were carried out in a spherical flow in order to measure a computational

* Corresponding author.

E-mail address: ohnishi@rhd.mech.tohoku.ac.jp (N. Ohnishi).

efficiency of our code, and the obtained light curve and emission spectrum with a simple expanding model are presented.

The organization of this paper is as follows. In the next section, we present numerical modeling of radiative transfer in this study. A simple model of relativistic expanding flow is introduced in Section 3 for examining an initial value problem based on relativistic jet solution. In Section 4, computational efficiency of our parallelized Monte Carlo code is assessed with a large number of sample particles aiming to show a feasibility of future large-scale computing. Physical interpretation of the obtained light curve and spectrum is also addressed in Section 5 to validate our numerical modeling. Then, we conclude this paper in Section 6.

2. Numerical modeling of radiative transfer

2.1. Basic equation

We calculate photon transport in a background flowfield in order to simulate gamma-ray flash from a relativistic jet. Therefore, we need to solve the radiative transfer equation including gamma-ray regime. Radiative transfer equation is written by

$$\left(\frac{1}{c} \frac{\partial}{\partial t} + \boldsymbol{\Omega} \cdot \nabla\right) I(\mathbf{r}, \boldsymbol{\Omega}, \nu, t) = j(\nu, T) + \frac{\rho(\mathbf{r}, t)}{4\pi} \iint \sigma(\nu) I(\mathbf{r}, \boldsymbol{\Omega}', \nu', t) \phi(\boldsymbol{\Omega}', \boldsymbol{\Omega}, \nu', \nu) d\nu' d\boldsymbol{\Omega}' - [k(\nu) + \sigma(\nu)] \rho(\mathbf{r}, t) I(\mathbf{r}, \boldsymbol{\Omega}, \nu, t), \quad (1)$$

where $I(\mathbf{r}, \boldsymbol{\Omega}, \nu, t)$ is the specific intensity as a function of the position \mathbf{r} , the traveling direction $\boldsymbol{\Omega}$, the photon frequency ν , and the time t . The variables j , k , ρ , and σ are the emissivity, the absorption cross-section, density, and the scattering cross-section, respectively. The emissivity j depends on the matter temperature T . The scattering kernel $\phi(\boldsymbol{\Omega}', \boldsymbol{\Omega}, \nu', \nu)$ is defined by the incident direction $\boldsymbol{\Omega}'$, the incident frequency ν' , the scattered direction $\boldsymbol{\Omega}$, and the scattered frequency ν . Note that if the scattering is isoenergetic such as Thomson scattering, $\nu' = \nu$.

In order to assess radiation transfer in scattering media, we need to solve the differential–integral equation (1) for I . However, since I depends on seven independent variables of three spaces, two directions, frequency, and time, it is difficult to obtain analytical solution. Even if we numerically try to solve the radiative transfer equation using finite difference manner, solution cannot be obtained in a practical resolution with reasonable computational costs. Therefore, in this work, we employ Monte Carlo method that is relatively facile to solve the radiative transfer equation including scatterings.

2.2. Monte Carlo method

Monte Carlo method is a technique that stochastically solves the transfer equation by tracking a large number of particles. Using Monte Carlo method, we can obtain an approximate solution of the transfer equation with reasonable computational costs. The remains of this section are devoted to describe the physical elements and numerical procedures of our Monte Carlo code.

2.2.1. Packet setting

A cluster of photons having single frequency is considered as a sample particle used in Monte Carlo method. Hereafter, we call it as packet. The packet has energy of $\epsilon(\nu) = nh\nu = nE$, where h is

Planck constant, and n is the number of photons in the packet. The emission coefficient is given by bremsstrahlung

$$j(\nu, T) d\nu = \frac{32\pi}{3} \left(\frac{2\pi}{3k_B T m_e}\right)^{1/2} \frac{Z^2 e^6}{m_e c^3} N_+ N_e e^{-h\nu/k_B T} d\nu, \quad (2)$$

where k_B , m_e , Z , e , c , N_+ , and N_e , are Boltzmann constant, electron mass, atomic number, elementary charge, speed of light, ion number density, and electron number density, respectively [19]. No line emission is included in the present paper. For the bremsstrahlung emission, emission power $\dot{\epsilon}$ at any position is described as the spectral integration of the emission coefficient given by

$$\dot{\epsilon} = \int_0^\infty j(\nu, T) d\nu = \frac{32\pi}{3} \left(\frac{2\pi k_B T}{3m_e}\right)^{1/2} \frac{Z^2 e^6}{m_e c^3 h} N_+ N_e. \quad (3)$$

The total emission power $\dot{\epsilon}$ over the entire flowfield can be obtained as a product of $\dot{\epsilon}$ and the total cell volume. Setting N as the number of packet emitted during Δt , the holding energy for single packet in a certain simulation step is given by

$$\epsilon_0 = \frac{\dot{\epsilon}}{N} \Delta t. \quad (4)$$

Since ϵ_0 is the energy in comoving frame (CMF), we need to transform it to that in observed frame (OF) in order to move the packets in a free path. We also randomly set initial frequency of packet ν_0 in the CMF within the range from 10^{13} to 10^{22} Hz, and transform it to that in the OF as well.

We randomly set the initial position of the emitted photon in the entire flowfield using random numbers. Also, the initial direction of the photon is set by two random numbers with the assumption of isotropic emission in the CMF; the initial direction vector $\boldsymbol{\Omega}_0 = (\sin\theta\cos\phi, \sin\theta\sin\phi, \cos\theta)$ can be expressed by

$$\cos\theta = 1 - 2z_1, \quad (5)$$

$$\phi = 2\pi z_2, \quad (6)$$

where z_1 and z_2 are random numbers for the direction. After the initial packet position is set in the OF, the traveling direction $\boldsymbol{\Omega}_0$ in the CMF is Lorentz-transformed using the flowfield (background) velocity at the corresponding position to obtain the direction vector $\boldsymbol{\Omega}$ in the OF. Using the direction $\boldsymbol{\Omega}$ and the flowfield velocity \mathbf{v} , the Lorentz-transformed frequency ν and packet energy $\epsilon(\nu)$ are given by

$$\nu = \nu_0 \frac{\sqrt{1 - (v/c)^2}}{1 - \boldsymbol{\Omega} \cdot \mathbf{v}/c}, \quad (7)$$

$$\epsilon(\nu) = \epsilon_0 \frac{\sqrt{1 - (v/c)^2}}{1 - \boldsymbol{\Omega} \cdot \mathbf{v}/c}, \quad (8)$$

respectively, in the OF.

2.2.2. Scattering and absorption of optical ray

In the Monte Carlo sequence, photons should be categorized into some energy groups because they have different types of scattering cross-sections depending on their energy regime. We categorize them into two groups in this paper, and the lower-energy photons are hereafter called ‘optical’, while the higher-energy group is expressed by ‘gamma ray’. In this work, we set the absorption cross-section for optical ray using Kirchhoff’s law

$$\frac{j(\nu, T)}{\rho k_0(\nu)} = \frac{2h\nu^3}{c^2} e^{-h\nu/k_B T}. \quad (9)$$

Total cross-section of the Thomson scattering is given by

$$\sigma_T = \int d\sigma(\mathbf{\Omega}') = \frac{8\pi}{3} r_e^2, \quad (10)$$

where r_e is the classical electron radius. We estimated the electron number density n_e by assuming that the species involved in the background is only fully-ionized helium gas. Therefore, we can determine the mass scattering cross-section σ_0 for optical ray as $\sigma_0 = \sigma_T n_e / \rho$. Since the above cross-sections are defined in the CMF, they should be Lorentz-transformed for free path estimation in the OF

$$\sigma = \sigma_0 \frac{\sqrt{1 - (v/c)^2}}{1 - \mathbf{\Omega} \cdot \mathbf{v}/c}, \quad (11)$$

$$k(\nu) = k_0(\nu) \frac{\sqrt{1 - (v/c)^2}}{1 - \mathbf{\Omega} \cdot \mathbf{v}/c}.$$

The optical ray is scattered or absorbed after traveling the free path δs . These events are simpler to be considered in the OF than the CMF. When the random number z holds $z < \sigma/(\sigma + k(\nu))$, the event is scattering; otherwise it is regarded as absorption. In the Thomson scattering, if the incident light is scattered, the energy of it in the CMF is fully transferred to the scattered light, so that $E'_0 = E_0$, where E'_0 is the post-scattering energy. The scattered angle and direction are determined by the direction vector of the incident light $\mathbf{\Omega}_0$ in the CMF. If the absorption to the matter occurs, we assume that the absorbed energy is quickly re-emitted as a new optical ray. The direction of the re-emitted light $\mathbf{\Omega}'_0$ is isotropic in the CMF, so that $\cos\theta = 1 - 2z_1$ and $\phi = 2\pi z_2$, where θ is the scattering angle. We also reset the energy E'_0 from $j(\nu, T)$. The post-event variables $\mathbf{\Omega}', E'$, and ϵ' in the OF are transformed from $\mathbf{\Omega}'_0, E'_0$, and ϵ'_0 in the CMF, respectively.

2.2.3. Scattering and absorption of gamma ray

The gamma ray leads to the Compton scattering or photoelectric absorption by interaction with the matter after free traveling in a certain distance. The gamma-ray free path is determined by cross-sections of these events and the matter density. If the gamma ray is scattered or absorbed, its energy is transferred to the scattered light and the matter, and finally to the optical ray. Generally, the cross-sections for the Compton scattering and the photoelectric absorption depend on the incident light energy. Therefore, we should care about the gamma-ray energy $E_0 = h\nu_0$ in the CMF in order to obtain these cross-sections.

The scattering cross-section in the CMF can be estimated by integrating the Klein–Nishina formula for solid angle

$$\frac{\partial \sigma_{KN}}{\partial \mathbf{\Omega}}(E_0, \mathbf{\Omega}) = \frac{1}{2} r_e^2 \left\{ f_c(E_0, \theta) - f_c^2(E_0, \theta) \sin^2 \theta + f_c^3(E_0, \theta) \right\}, \quad (12)$$

where f_c is given by $f_c = 1/[1 + x(1 - \cos\theta)]$ for $x = E_0/(m_e c^2)$. The mass cross-section σ_0 is determined with the above cross-section,

the mean mass \bar{m} , and the mean atomic number \bar{Z} in the given cell, so that $\sigma_0 = \sigma_{KN} \bar{Z} / \bar{m}$, where $\sigma_{KN}(E_0) = \int \partial \sigma_{KN} / \partial \mathbf{\Omega}(E_0, \mathbf{\Omega}) d\mathbf{\Omega}$.

Because it is difficult to derive the absorption cross-section $k_0(E_0)$ in the CMF, we approximate it by power of E_0 based on the absorption cross-section of the reference energy. In this paper, we use 100 keV as the reference, and the absorption cross-section is represented by

$$k_0(E_0) = k_0^{100} \left(\frac{E_0}{100 \text{ keV}} \right)^{-3}, \quad (13)$$

where k_0^{100} is the absorption cross-section for 100-keV gamma ray. The reference cross-section is obtained from the fraction of each species f_i and the corresponding absorption cross-section $k_{0,i}^{100}$ for 100-keV gamma ray as follows:

$$k_0^{100} = \sum_i f_i k_{0,i}^{100}. \quad (14)$$

The fraction f_i is determined by the composition in each cell, and the experimental values are used for $k_{0,i}^{100}$. Transforming k_0 and σ_0 in the CMF to the OF, the corresponding values k and σ are obtained, respectively.

After traveling the free path δs in the direction $\mathbf{\Omega}$, the gamma ray is scattered or absorbed. Probability of the events is proportional to each cross-section in the OF. Thus, if the random number fulfills the condition that $z < \sigma(E)/(\sigma(E) + k(E))$, the Compton scattering occurs, but otherwise the photoelectric absorption does. We then should consider these events in the CMF.

If the event is the Compton scattering, the scattering angle θ can be determined by random number z with Klein–Nishina formula

$$z = \frac{1}{\sigma_{KN}(E_0)} \int_0^\theta \frac{\partial \sigma_{KN}(E_0, \theta')}{\partial \theta'} d\theta'. \quad (15)$$

Moreover, the angle ϕ in a plane perpendicular to $\mathbf{\Omega}_0$ is randomly chosen by $\phi = 2\pi z$. Since a part of energy of the incident light is transferred to the electron, fraction of the incident light energy to the kinetic energy of the scattered electron is introduced by f_c for energy conservation in the CMF. In order to keep number of particles through the events, all the energy of the incident packet is transferred to either the scattered light or the scattered electron, but the probability of the destination is proportional to the fraction f_c .

In the case that $z < f_c$, the energy of the scattered light is $E'_0 = f_c E_0$. So, we have to determine the traveling direction $\mathbf{\Omega}'_0$ from $\mathbf{\Omega}_0$, θ , and ϕ . Using the direction vector $\mathbf{\Omega}'$ in the OF transferred from $\mathbf{\Omega}'_0$, the energy of the scattered light E' in the OF becomes $E' = E'_0 \sqrt{1 - (v/c)^2} / (1 - \mathbf{\Omega}' \cdot \mathbf{v}/c)$, and the packet energy $\epsilon' = \epsilon'_0 \sqrt{1 - (v/c)^2} / (1 - \mathbf{\Omega}' \cdot \mathbf{v}/c)$. In the case that $z > f_c$, the packet energy is transferred to the scattered electron. Because the electron free path is much shorter than that of light, we assume that the electron is quickly thermalized, and all the electron energy is used to generate a new optical ray. We also do not take effect of electron spectra into account by a proper sampling of electron energies for simplicity. We should deal with this effect in a realistic simulation.

If the event is the photoelectric absorption, the background atom is ionized by the incident light. A part of energy is consumed for the ionization, and the residual energy is transferred to the kinetic energy of the liberated electron and the ion. However, one can consider that the electron and ion are quickly thermalized as well as the scattering event. The ion rapidly returns to the former state and emits a light which has much lower energy than the original.

Therefore, in the case of the photoelectric absorption, all the energy is assumed to be transferred to the optical ray, i.e., $\epsilon'_0 = \epsilon_0$. This optical ray is also emitted isotropically in the CMF, and its frequency is randomly chosen as obeying Planck function.

2.2.4. Free path of photon

The free path of photon δs between the events depends on the cross-sections in the OF. The optical depth of the matter corresponding to δs is given by

$$\tau = (\sigma(E) + k(E))\rho\delta s. \quad (16)$$

The free path of the photon is determined by probabilistic manner using τ . If the radiative transfer equation includes only dissipation term relevant to the absorption and scattering, it is reduced to the following form:

$$\frac{dI(E, \tau)}{d\tau} = -I(E, \tau).$$

Therefore, the incident intensity $I(E, 0)$ drops exponentially with τ

$$I(E, \tau) = I(E, 0)e^{-\tau}. \quad (17)$$

This shows the probability that the photon freely travels to τ can be represented by

$$p(\tau) = \frac{I(E, \tau)}{I(E, 0)} = e^{-\tau}. \quad (18)$$

When the uniform random number for the free path equals to the integrated probability in the following form:

$$z = \int_0^\tau p(\tau')d\tau',$$

the free optical depth is readily expressed with it

$$\tau = -\ln(1 - z). \quad (19)$$

Therefore, the flying distance of the photon δs is given by

$$(\sigma(E) + k(E))\rho\delta s = -\ln(1 - z). \quad (20)$$

Also, the time duration $\delta t = \delta s/c$ takes while the packet travels in δs . The time t for the packet should be incremented to $t + \delta t$ between the events.

2.2.5. Observed time

Reaching the boundary of the flowfield and escaping from there, the photon is added to the observed signal. However, the observed time is different for the escaped position of each photon, so we need to translate the escaped time t_{out} to the observed time t_{obs} .

As shown in Fig. 1, the observed time of the photon that escapes at t_{out} from the position \mathbf{R} in the direction $\boldsymbol{\Omega}$ is written by

$$t_{\text{obs}} = t_{\text{out}} + \frac{\sqrt{L^2 + R^2 - 2\mathbf{L} \cdot \mathbf{R}}}{c}, \quad (21)$$

where \mathbf{L} is the distance vector from the center of the flowfield to the observer, and R is the absolute value of \mathbf{R} , i.e., the distance from the center of the flowfield. Since the direction of the escaped photon $\boldsymbol{\Omega}$ can be expressed by $\boldsymbol{\Omega} = (\mathbf{L} - \mathbf{R})/|\mathbf{L} - \mathbf{R}|$, the inner product in Eq. (21) is written with $\boldsymbol{\Omega}$

$$\mathbf{L} \cdot \mathbf{R} = R^2 + |\mathbf{L} - \mathbf{R}|\boldsymbol{\Omega} \cdot \mathbf{R}. \quad (22)$$

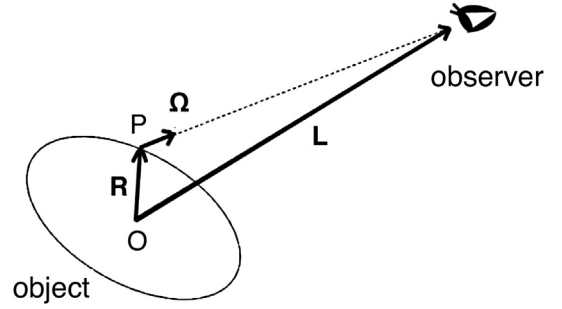


Fig. 1. Positional relation among object center, escape point, and observer.

With the assumption that the absolute value of \mathbf{L} , L , is much larger than R , we can approximate the observed time as follows:

$$\begin{aligned} t_{\text{obs}} &= t_{\text{out}} + \frac{\sqrt{L^2 + R^2 - 2(R^2 + |\mathbf{L} - \mathbf{R}|\boldsymbol{\Omega} \cdot \mathbf{R})}}{c} \\ &= t_{\text{out}} + \frac{L}{c} \sqrt{1 - \left(\frac{R}{L}\right)^2 - \frac{2|\mathbf{L} - \mathbf{R}|\boldsymbol{\Omega} \cdot \mathbf{R}}{L^2}}, \quad (23) \\ &\approx t_{\text{out}} + \frac{L}{c} \left(1 - \frac{|\mathbf{L} - \mathbf{R}|\boldsymbol{\Omega} \cdot \mathbf{R}}{L^2}\right) \\ &\approx t_{\text{out}} + \frac{L}{c} - \frac{\boldsymbol{\Omega} \cdot \mathbf{R}}{c} \end{aligned}$$

Although the above equation includes the term of L/c , we are not concerned with the concrete distance between the object and the observer. In terms of the purpose to plot a light curve, we can neglect this term with the assumption that the center of the flowfield does not move against the observer. So, in this paper, we use the observed time defined by

$$t_{\text{obs}} = t_{\text{out}} - \frac{\boldsymbol{\Omega} \cdot \mathbf{R}}{c}. \quad (24)$$

As found in the above discussion, \mathbf{R} does not need a constant value. Thus, this formula can be applied for non-spherically symmetric flowfield. We consequently obtain the luminosity by summing of packet energy ϵ_v that escapes from the flowfield within $[t_{\text{obs}}^n, t_{\text{obs}}^{n+1}]$, where the superscript n denotes the simulation step.

3. Background flowfield

Three-dimensional Monte Carlo simulations of radiative transfer are carried out based on hydrodynamical data of the relativistic jet [5] in which the Thomson scattering dominates compared to absorption. Using axial data from the MHD simulation, as initial conditions, we prepared one-dimensional spherically expanding flowfield that transits from optically thick to thin. The initial conditions of this relativistic flowfield are displayed in Fig. 2.

Our Monte Carlo code takes into account the Thomson and Compton scatterings and the absorption with regarding the emitted photons.

For the background flowfield, the polar coordinate system is used. In each computational cell, physical quantities are assumed to be uniform and constant at each cell within the time step Δt . Photons experience several cells in Δt when they travel especially in the optically thin region. In this paper, the background profiles change with time increment by following a simple model described below, but no constraint appears for time step because of no characteristic wave in the model. Therefore, we set time step to $\Delta t_{n+1} = \Delta t_n / (1 - n_{\text{nocol}})$

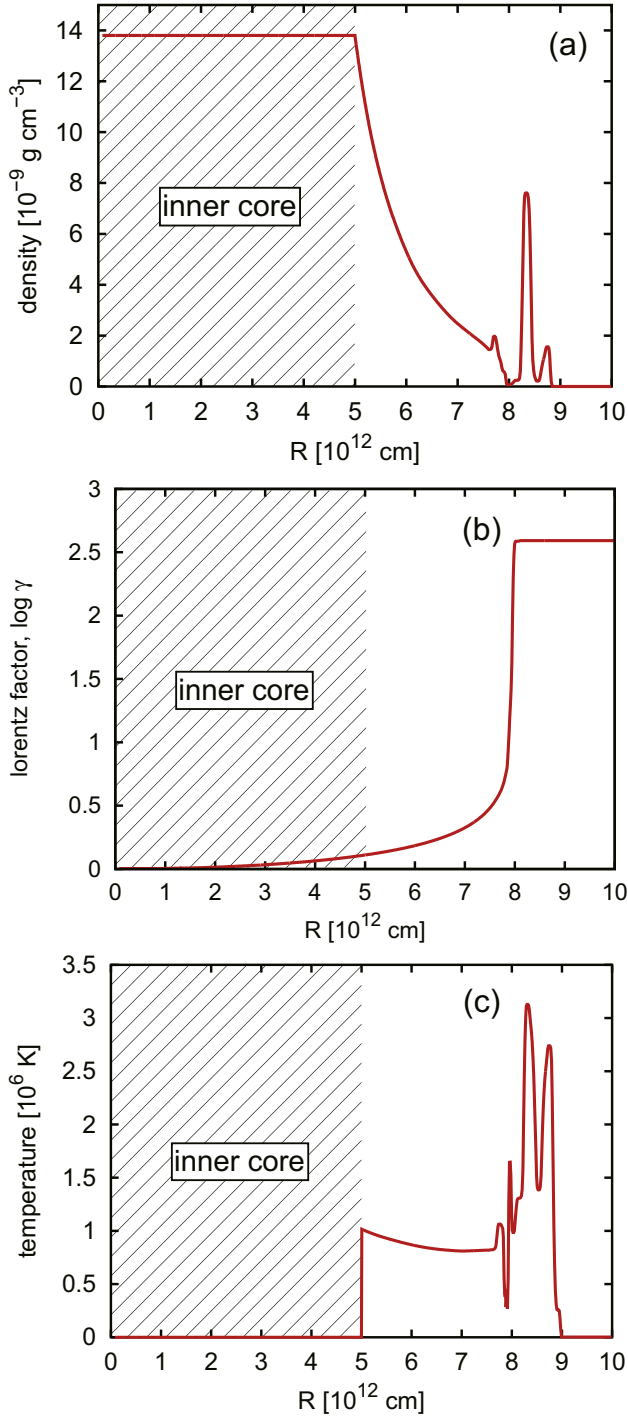


Fig. 2. (a) Initial density profile, (b) initial Lorentz factor profile, and (c) initial temperature profile obtained from the relativistic jet simulation [5].

$n_{\text{all}} \times 0.1$), where n_{nocol} is the number of photons that never collide during one time step, and n_{all} is the number of all photons in that step.

From single snapshot of the hydrodynamical data (Fig. 2), the background flowfield is obtained by solving the continuity equation in spherical Lagrangian coordinate [20] under the assumption of constant velocity expansion

$$dm = 4\pi r^2 dr \gamma \rho, \quad (25)$$

where m is the mass coordinate, r is the radial coordinate, and γ is the Lorentz factor defined by the flow velocity v

$$\gamma = \frac{1}{\sqrt{1 - (v/c)^2}}. \quad (26)$$

If the radial coordinate constantly expands with the initial position r_0 and flow velocity v as follows:

$$r = r_0 + vt, \quad (27)$$

the density is determined by Eq. (25). Assuming that the radiation pressure dominates in the flowfield, radiation pressure p_v may obey the polytropic gas relation with the obtained density

$$p_v = K\rho^\Gamma, \quad (28)$$

where K is the constant determined by the initial condition, and Γ is the polytropic constant; $\Gamma = 4/3$ in this paper. The pressure is also related to the temperature T through the equation of blackbody radiation

$$3p_v = \frac{4\sigma T^4}{c}. \quad (29)$$

As the spherical flow expands with the relativistic velocity, the density and the pressure rapidly drop down. This leads to the photon break-out due to the transition from opaque flow to transparency. In the later time, however, the emission cannot sustain large photon generation because the temperature falls with the pressure.

Although pair production is actually dominant as absorption process in high-energy gamma ray, we assume that it rarely occurs

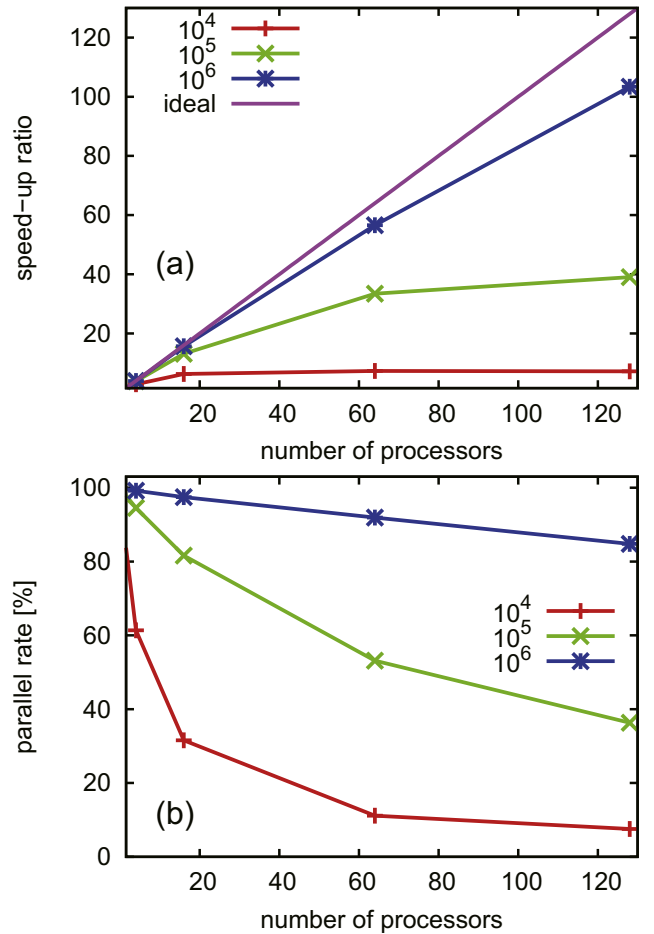


Fig. 3. (a) Speed-up ratio and (b) parallel rate measured by the developed Monte Carlo code.

and the Compton scattering is still dominant because the atomic number is low in this model [21]. Similarly, gamma–gamma absorption is also not taken into account in this simulation. These effects should be treated in a realistic simulation.

4. Parallel computation

Since a large number of packets and long-term tracking in a scattering medium are required for an accurate prediction of light curves and emission spectra with less statistical errors, Monte Carlo simulation needs huge computational loads. Our parallelized Monte Carlo code achieves a high parallel efficiency that helps us to obtain solutions in a practical computational time. Computational speed-up ratio S_n and parallel rate P are defined by

$$S_n = \frac{T_1}{T_n}, \quad (30)$$

$$P = \frac{T_p}{T_{\text{tot}}}, \quad (31)$$

respectively, where T_1 , T_n , T_p , and T_{tot} denote time of single computing, time of parallel computing with n processors, time of computing the parallelized part, and time of computing all the parts, respectively. The parallel computing was carried out using up to 128 cores on the SGI AltixUV1000 equipped with maximum 512

cores of Intel Xeon X7560 at the Institute of Fluid Science, Tohoku University, with Message Passing Interface (MPI) library.

Speed-up ratio increases as the number of particles increasing, where the number is defined by particles added in a single time step (Fig. 3(a)). When the number of particles is 10^6 , the Monte Carlo computing is highly accelerated in contrast that the parallel computing speed is not so faster than single computing speed with the number of particles of 10^4 . However, the parallel rate decreases with increasing number of processors (Fig. 3(b)) because the parallelized part for each CPU decreases with increasing the number of processors. On the other hand, since the parallelized part is devoted to track photons assigned to each CPU, the fraction of it in the entire computation increases with increasing the number of particles.

5. Light curve and spectrum

We conducted radiative transfer computations in the relativistic flow with the simple expanding model and obtained the light curve and the spectrum of the photon number flux (Fig. 4). In this case, 10^5 of packets were added in a single time step. The light curve is found in a power-law with t^{-3} . Observed light curves usually show the feature that decreases linearly with time in double logarithm plot as found here [22]. Moreover, the escaped photon energy after the peak is close to total emission power because the flowfield becomes optically thin. In such a transparent regime, emission flux should be proportional to $T^4 S$, where S is the emission area. The term of T^4 is determined from p_ν by Eq. (29) and is then proportional to ρ^Γ from Eq. (28). Since the constant expansion $r \propto vt$ is assumed, ρ and S proportionally grow with $(vt)^{-3}$ and $(vt)^2$, respectively. Considering

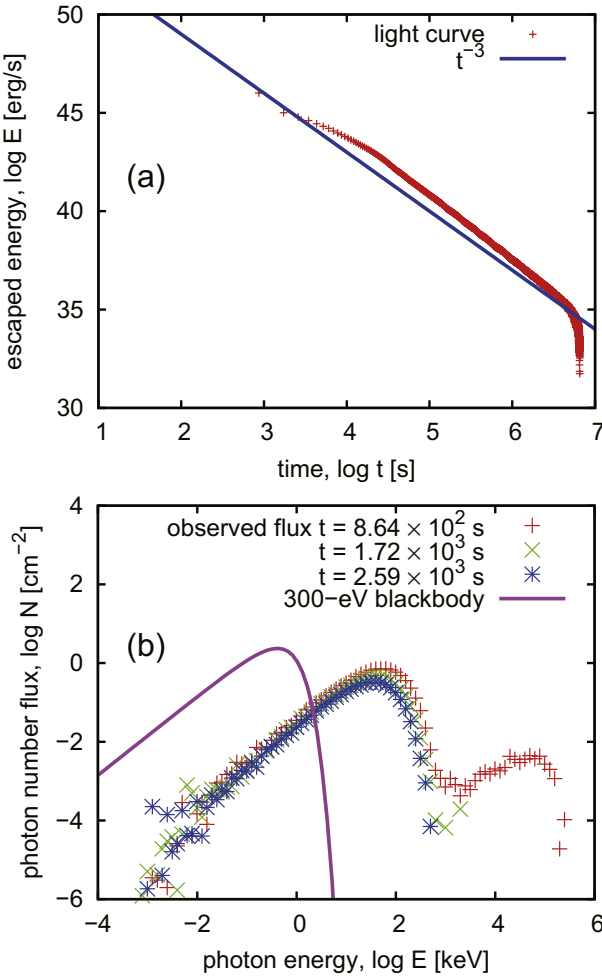


Fig. 4. Obtained (a) light curve and (b) spectrum of photon number flux from the spherically expanding relativistic flow.

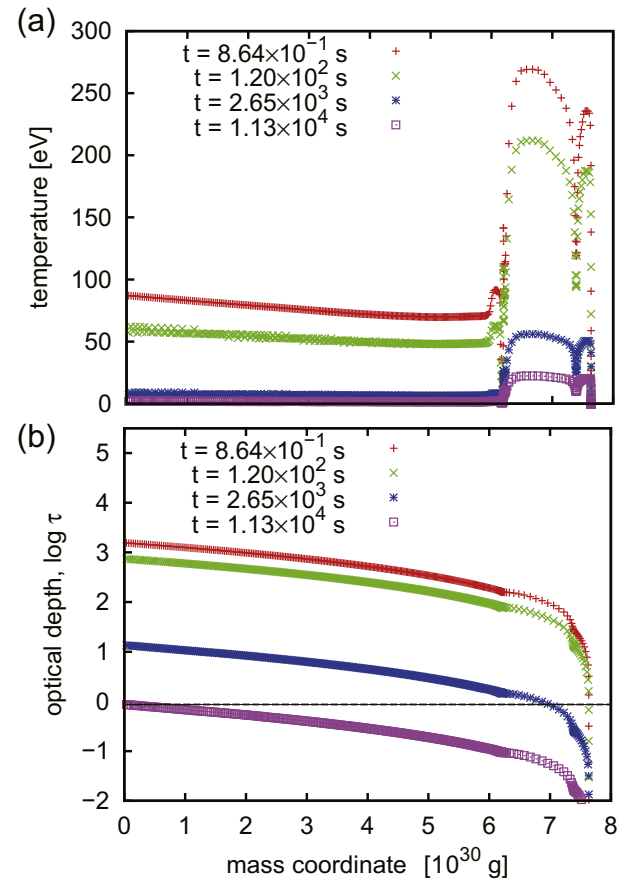


Fig. 5. Time evolution of (a) temperature and (b) optical depth in the mass coordinate.

that $\Gamma = 4/3$, we obtain the relation of $T^4 S \propto t^{-2}$. After differentiating this with respect to t , we can estimate that time variation of the escaped photon energy is proportional to t^{-3} . In Fig. 4(a), a part of the light curve is not proportional to t^{-3} from 10^3 to 10^4 s. It may come from the fact that the flowfield changes from optically thick to intermediate in that duration. As shown in Fig. 5, the optical depth τ is unity in the high temperature region at around 10^4 s, so that almost all of emitted energy is radiated as the escaped energy.

The spectrum of photon number flux is compared with the Planck distribution of 300 eV which is a typical value in the initial high temperature region. The number flux is defined by

$$\frac{N_{\text{esc}}/\Delta t}{4\pi R^2} \times \frac{R^2}{d^2}, \quad (32)$$

where N_{esc} is the escaped photon number and d denotes the distance between the outer radius and the observer (10 Mpc). We can find that the peak energy of the spectrum is almost 10^2 higher than that of the Planck distribution because of the Doppler boosting owing to the relativistic flow velocity. Higher-energy photons are also found, which may come from the inverse Compton scattering. Time evolution of the arbitrarily selected photons during the single time step at $\Delta t = 550$ s shows that the photon energy increases

repeating the scatterings in the relativistic flow as shown in Fig. 6. This may result from high Lorentz factor at near edge of the flowfield, in which the flow velocity is almost speed of light. High density in such region is also responsible for generating high-energy photons because the photons are easily to be scattered many times. Note that Fig. 6 is a close-up view for drawing scattering trajectories, and the photons continue to travel after this time step.

6. Conclusion

Parallel Monte Carlo code simulating radiative transfer in a relativistic flow has been developed to examine a feasibility that a relativistic jet formed around a collapsing massive star that becomes an engine of GRBs. The code can describe photon traveling over the flow in the OF and scattering and absorption processes in the CMF in order to figure light curves and spectra found by a distant observer. High parallel efficiency was achieved with the developed code, and preliminary simulations were carried out with a simple background model of relativistic spherical flow.

Since a large number of particles is required for obtaining reliable results with the Monte Carlo code with less statistical error, parallel computing is a lifeline toward future large-scale computations coupled with a flowfield given by multi-dimensional hydrodynamical simulation. We parallelized the Monte Carlo code using MPI, and performance of parallel computing was measured with over a hundred of processors. As a result, the parallel efficiency approaches to ideal one when 10^6 particles are added in the single simulation step while it becomes worse with the smaller number of particles because the fraction of the parallelized part, i.e., photon tracking part in a computational sequence decreases for that case. In other words, the developed code must show higher performance with a larger number of particles for attaining an accurate prediction from a long-term relativistic flows on a massively parallel computer system.

The preliminary simulation of radiative transfer with the simple expansion model produces gamma-ray emission through the Doppler boosting and the inverse Compton scattering even with the initial matter temperature of ~ 300 eV, which is given by a snapshot of the preprocessed relativistic jet simulation. The obtained light curve shows a power-law feature widely found in the actual observation of GRBs. As the background matter expands, the observed emission grows up due to a transition in the post-shock dense region to diffusive regime with deviating from the power-law. However, at the later time, the light curve obeys the power-law again because photons freely travel away in the entire flowfield. The high-energy plateau is also found in the obtained spectra at the early time because some optical rays, which first travel inward and is scattered to outward, are pumped up by the inverse Compton scattering within the dense region.

The relativistic jet from the collapsing massive star has high Lorentz factor flow in which the velocity is almost speed of light. Although such flowfield can produce gamma rays in the processes as shown in this paper, bridging data between the hydrodynamic simulation and the Monte Carlo transfer is not straightforward since a simple interpolation of the flow velocity fails due to the causality break resulting from the round-off error. Nevertheless, we should address the coupling computation with the relativistic flow because it must arouse a controversy of the GRB origin.

References

- [1] S.E. Woosley, *Astrophys. J.* 405 (1993) 273.
- [2] B. Paczynski, *Astrophys. J.* 494 (1998) L45.
- [3] S.E. Woosley, J.S. Bloom, *Annu. Rev. Astron. Astrophys.* 44 (2006) 507.
- [4] P. Meszaros, *Rep. Prog. Phys.* 69 (2006) 2259.

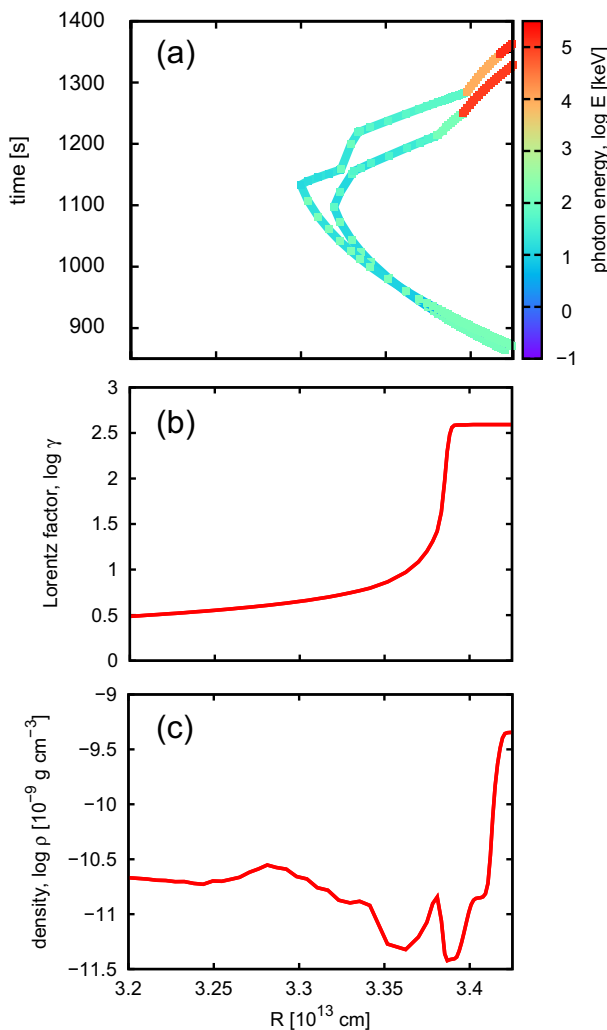


Fig. 6. (a) Time evolution of trajectory and energy of arbitrarily selected two photons that gain extremely high energy through multiple scatterings and profiles of (b) Lorentz factor and (c) density in a single time step of 850–1400 s.

- [5] H. Nagakura, H. Ito, K. Kiuchi, S. Yamada, *Astrophys. J.* 731 (2011) 80.
- [6] J.K. Cannizzo, N. Gehrels, E.T. Vishniac, *Astrophys. J.* 601 (2004) 380.
- [7] H. van Eerten, W. Zhang, A. Macfadyen, *Astrophys. J.* 722 (2010) 235.
- [8] A. Mizuta, T. Yamasaki, S. Nagataki, S. Mineshige, *Astrophys. J.* 651 (2006) 960.
- [9] A. Mizuta, M.A. Aloy, *Astrophys. J.* 699 (2009) 1261.
- [10] D. Lazzati, B.J. Morsony, M.C. Begelman, *Astrophys. J.* 700 (2009) L47.
- [11] A. Mizuta, S. Nagataki, J. Aoi, *Astrophys. J.* 732 (2011) 26.
- [12] K. Ioka, K. Murase, K. Toma, S. Nagataki, T. Nakamura, *Astrophys. J.* 670 (2007) L77.
- [13] A.A. Abdo, M. Ackermann, M. Ajello, et al., *Astrophys. J.* 706 (2009) L138.
- [14] F. Ryde, M. Axelsson, B.B. Zhang, et al., *Astrophys. J. Lett.* 709 (2010) L172.
- [15] A. Pe'er, F. Ryde, *Astrophys. J.* 732 (2011) 49.
- [16] K. Maeda, *Astrophys. J.* 644 (2006) 385.
- [17] A. Suzuki, T. Shigeyama, *Astrophys. J.* 719 (2010) 881.
- [18] L.B. Lucy, *Astron. Astrophys.* 429 (2005) 19.
- [19] Y.B. Zel'dovich, Y.P. Raizer, *Physics of Shock Waves and High-temperature Hydrodynamic Phenomena*, Dover, 2002.
- [20] Y.A. Urzhumov, *Gravit. Cosmol.* 8 (2002) 222.
- [21] G. Nelson, D. Reilly, in: D. Reilly, et al. (Eds.), Sec. 2 in *Passive Nondestructive Analysis of Nuclear Materials* (1991). LA-UR-90-732.
- [22] D.E. Reichart, *Astrophys. J.* 521 (1999) L111.